UCRL-10907
c.2

University of California

Ernest O. Lawrence Radiation Laboratory

TWO-WEEK LOAN COPY

This is a Library Circulating Copy which may be borrowed for two weeks. For a personal retention copy, call Tech. Info. Division, Ext. 5545

NEUTRON DOSIMETRY NEAR A BARE PULSED REACTOR

Berkeley, California

UCRL-10907
c.2

DISCLAIMER

This document was prepared as an account of work sponsored by the United States Government. While this document is believed to contain correct information, neither the United States Government nor any agency thereof, nor the Regents of the University of California, nor any of their employees, makes any warranty, express or implied, or assumes any legal responsibility for the accuracy, completeness, or usefulness of any information, apparatus, product, or process disclosed, or represents that its use would not infringe privately owned rights. Reference herein to any specific commercial product, process, or service by its trade name, trademark, manufacturer, or otherwise, does not necessarily constitute or imply its endorsement, recommendation, or favoring by the United States Government or any agency thereof, or the Regents of the University of California. The views and opinions of authors expressed herein do not necessarily state or reflect those of the United States Government or any agency thereof or the Regents of the University of California.

UCRL-10907

UNIVERSITY OF CALIFORNIA

Lawrence Radiation Laboratory
Berkeley, California

Contract No. W-7405-eng-48

NEUTRON DOSIMETRY NEAR A BARE PULSED REACTOR

Richard L. Lehman, Hiroaki Akagi, and Olga M. Fekula

July 15, 1963

NEUTRON DOSIMETRY NEAR A BARE PULSED REACTOR

Richard L. Lehman, Hiroaki Akagi, and Olga M. Fekula

Lawrence Radiation Laboratory
University of California
Berkeley, California

July 15, 1963

ABSTRACT

Nuclear track emulsion was exposed in and around human phantoms to pulsed U-235 fission neutrons at the outdoor burst site of the Sandia Pulsed Reactor Facility at Albuquerque, New Mexico. The phantoms were located at distances from 10 to 200 m from the reactor. Tracks in the developed emulsions were scanned in order to obtain the local differential proton track energy spectra at 10 locations in and around the phantoms. From this was calculated the local absolute differential tissue dose, the local thermal n, p tissue dose, and the local fast-neutron energy spectrum. The maximum and minimum tissue proton doses in rads per 10^{18} fissions were found to be 330 and 33 at 10 m, 45 and 5.9 at 25 m, 2.6 and 0.46 at 100 m, and 0.58 and 0.076 at 200 m.

NEUTRON DOSIMETRY NEAR A BARE PULSED REACTOR*

Richard L. Lehman, Hiroaki Akagi, and Olga M. Fekula

Lawrence Radiation Laboratory
University of California
Berkeley, California

July 15, 1963

I. INTRODUCTION

The validity of nuclear track emulsion for fast-neutron dosimetry has been examined in the case of plutonium-beryllium neutrons.[1] It was found that the absolute differential proton track energy spectrum could be obtained at various locations in and around human phantoms without a serious cost in time by use of a semiautomatic microscope and an electronic computer. This preliminary work was an attempt to answer the question: "How good is nuclear emulsion technique for analyzing and evaluating tissue dose from neutrons?" The present work is a second step in the attempt to answer this question.

Nuclear track emulsion in and around human phantoms was exposed to pulsed U-235 fission neutrons at the outdoor burst site of the Sandia Pulsed Reactor Facility (SPRF). The phantoms were placed at distances of 10, 25, 50, 100, and 200 m from the reactor. Tracks in the developed emulsions were scanned and analyzed in order to obtain the local differential proton tissue dose.

II. EXPERIMENTAL METHOD

The Reactor

The SPRF has been described by O'Brien.[2] The reactor is a bare metal oralloy assembly constructed in 1960. It was patterned after the Godiva reactors at Los Alamos and is basically a copy of Godiva II.[3] The SPR neutron emission is isotropic,[4] and the neutron spectrum is expected to be the same as that reported for Godiva I, which contains a somewhat higher percentage of low-energy neutrons than a pure U-235 fission spectrum.[5]

The reactor assembly was mounted on a rubber-tired trailer frame that held the reactor head 2 m above the ground. For at least 800 m in all directions from the outdoor burst site the terrain was flat. The nearest structure was the control-room building, 730 m distant from the burst site.

Over a two-day period, October 16 and 17, 1961, there were six separate bursts, each between the limits of 0.3 and 2.0×10^{16} fissions. The duration of the bursts was about 50μsec. The temperature in the reactor metal rose by 108°C during a 2.0×10^{16} fission burst.

The Phantom

The three human phantoms were identical right elliptical cylinders 20 by 36 cm by 60 cm high made of 0.65-cm polyethylene, and filled with water. During the reactor burst they stood atop their wooden packing crates 92 cm above the ground, at distances between 10 and 200 m from the reactor.

The Nuclear Emulsions

Ilford L4 600-μ emulsions were cut into four pieces 1 by 3/4 in. from an original piece 1 by 3 in., and each was wrapped with black paper and black tape. Each emulsion was sealed in a 20-mil polyvinyl packet with Kodak NTA type film. Five such packets were held normal to the source direction by use of fine copper wire inside the water-filled phantom at the midcenter plane.

Also five packets were placed around the outside of the phantom at the mid-center plane with cellulose tape. The orientation of the film packets may be seen in Fig. 1. The developing, fixing, and mounting procedures have been described previously, as has the semiautomatic track scanning and the analysis by electronic computer.[1] The Ilford films used here were manufactured 20 September, 1961 and were developed 1 November, 1961.

The Burst Exposure

The exposure routine may be seen in Table 1. Altogether 70 film packets were exposed in groups of 10 each in and around the phantoms. The film packets C-40 to C-59 were identical to the others, with the exception that the L.4 and NTA films were wrapped together by use of a single layer of 0.25-mm cadmium sheet.

III. RESULTS

Ilford emulsions

The proton recoil energy spectra in and around the human phantoms as computed from tracks scanned in the Ilford L.4 emulsions are presented in Tables 2 through 7. (The emulsions listed on each table follow the order shown in Fig. 1.) The values listed in the tables are $\Delta N/P\Delta E$, normalized to give $\Sigma(\Delta N/P\Delta E) = 10\ 000$. In this ΔN is the number of tracks in energy interval ΔE, and P is a geometry correction factor: the probability that a track of the given energy which originates in the emulsion will end in the emulsion. The normalization allows direct comparison of the spectra, channel by channel.

The values in Tables 2 through 7 have not been corrected for the sampling inefficiency for short tracks. Such corrections must be made in order to obtain useful dose information. It has been found[1] that the

empirically determined factor $f = 0.44E^{-2.3}$ corrects channels 5 through 9. The track spectrum in the 0- to 0.40-MeV region was estimated by plotting the tabulated values, and then extrapolating from the points of channels 13 and 14 through the corrected points of channels 5 and 6. An example of this procedure may be seen in Fig. 2. The theoretical proton recoil spectrum $N_p(E)$ in Fig. 3 was a useful guide for this extrapolation. It is a plot of

$$N_p(E) = \int_{\infty}^{E} \frac{N_n(E)\,\sigma(E)}{E}\,dE,$$

where $N_n(E)$ is the equation for the pure U-235 fission neutron spectrum, $\sinh(2E)^{1/2}\,e^{-E}$. Figure 3 also shows the theoretical proton recoil dose spectrum $D_p(E) = E \cdot N_p(E)$ in a hydrogenous detector that does not perturb the local neutron spectrum.

Table 8 lists the proton track data obtained from the Ilford emulsions. The measured track density was determined independently by a direct count of all track endpoints in depth within a standard field of view. This number was then halved. Approximately 500 tracks or 50 fields of view per emulsion were scanned, depending upon track density. The correct average proton track energy and the percent thermal n,p tracks were obtained directly from a plot(e.g., Fig. 2) of the corrected proton track spectrum. The emulsion proton dose is the product of the correct track density and the correct average proton energy. The product of the percent thermal n,p tracks, the correct track density, and the energy of the n,p tracks (0.60 MeV) gave the thermal n,p emulsion dose. The proton recoil emulsion dose is the difference between the total proton and the n,p dose.

The background track spectrum in the L.4 emulsions is given in Fig. 4. For comparison the theoretical proton spectrum of Fig. 3 is

superimposed upon it. The background spectrum was scanned from two films, D-55 and D-58, that accompanied the experimental films at all times except during the actual bursts. Two "spikes" distort the recoil proton distribution, one at 0.6 to 0.7 MeV, and the other at 1.2 to 1.5 MeV. The 0.6-MeV spike consists of nuclear protons from the $N^{14}(n,p)C^{14}$ reaction. The 1.3-MeV peak does not consist of protons, but rather of alpha-particle tracks of energy 5 to 6 MeV that are scanned as proton tracks. In nuclear emulsion, the range of a 5.5-MeV alpha particle equals that of a 1.3-MeV proton. We have previously observed that the alpha-track background of nuclear emulsions increases with time between manufacture and development. Therefore, it probably arises from contamination of the emulsion with minute quantities of alpha emitters during manufacture. No correction has been made for the background track density because the energy spectrum was similar to that in the experimental films, and the background track density was only 1.9×10^4 t/cm^3 or approximately 1% of the total track density in the experimental emulsions.

NTA emulsions

The total neutron response of the NTA films may be seen in Fig. 5. The field of view in these films was 0.00060 cm^2 when 450× magnification was used.

In addition, the net optical density of the NTA films was measured by a densitometer. The relative film densities are presented in Fig. 6. For comparison, the equivalent density from given exposures of control films to radium gamma rays in air is given. These exposures should be regarded as the "upper limit" of the total X-ray and gamma exposures (see Sec. 4).

IV. DISCUSSION

The properties of nuclear track emulsion that make it particularly suitable for neutron dosimetry may be briefly listed: (a) It does not perturb the local neutron spectrum, (b) it records the recoil events in space, (c) it is continuously sensitive, (d) it has a low gamma sensitivity, (e) it requires no attached electronic apparatus, (f) many simultaneous measurements can be taken, and (g) it makes a permanent record. The major disadvantages of this dosimeter are (a) the time delay of several days between exposure, scanning and analysis; and (b) the restricted range of sensitivity: 0.40 to 20 MeV.

Used as described in this paper, nuclear emulsion is a fast-neutron dosimeter that yields the absolute differential proton tissue dose. In addition the general form of the local fast-neutron spectrum may be obtained.

1. Average energy of the proton track spectra

The average energy of the corrected track spectra remained remarkably constant at 0.77 to 0.80 MeV at the various distances. At 10 and 25 m the high average energy at the front surface was balanced by a low average energy at the back surface. But at 100 and 200 m, the average was very close to 0.78 MeV at all positions in and around the phantom. This reflects an isotropic exposure at the greater distances—and a remarkably constant local fast-neutron spectrum. The average proton-recoil energy in the cadmium-covered films was about 0.85 MeV, precisely the value computed theoretically from the curve of Fig. 3.

2. Calculation of the absolute total neutron dose in tissue

In each case, the proton recoil emulsion dose (in Table 8) is increased by 1.86, the ratio of the atomic density of hydrogen in tissue to that

in L.4 emulsion. To this is added 0.406 times the thermal n,p emulsion dose. The sum is the total proton tissue dose presented in Table 9. The factor 0.406 is the ratio of the nitrogen atomic density in tissue to that in L.4 emulsion.

3. The absolute differential proton tissue dose

Three operations on the plots of the emulsion proton spectra were carried out in order to obtain the differential tissue dose: (a) The area of the thermal n,p peak at 0.6 MeV was reduced by a factor of 4.6, (e.g., 1.86/0.406), (b) each point was multiplied by E, its abscissa value, and (c) the entire area under the curve was normalized to equal the total proton tissue dose. Selected examples are presented in Figs. 7 through 11. For comparison, the theoretical dose curve from Fig. 3 is superimposed upon each of these figures.

The fractional areas of certain energy intervals under these curves have been measured numerically. This more detailed information is presented in Table 10 for certain of the Ilford films.

4. Estimate of the local fast-neutron spectrum

The local fast-neutron spectra may be obtained as follows: A smooth curve is drawn through the corrected points of the proton recoil spectrum (Fig. 2). At the desired energies E_i, the slope of the smooth curve is measured or calculated. The product of the slope and $E_i/\sigma(E_i)$, where $\sigma(E_i)$ is the cross section for elastic collision of neutrons of energy E_i with hydrogen nuclei, gives one point of the neutron spectrum. A local neutron spectrum inside the phantom at 200 m is given in Fig. 2.

5. The neutron dose from the NTA response

It has been found in NTA dosimeter film that the fast-neutron dose in rems from a mock-fission neutrons source may be obtained by use of the

factor 6.7 tracks/field per rem.[6] In this an RBE of 10 is assumed; i.e., 1 rad = 10 rems. Table 9 shows the NTA tissue-doses and the ratio of these doses to the respective Ilford L.4 film doses. The agreement is generally within 10% at 10 and 25 m, but at the greater distances the NTA response drops to about 70% of the Ilford response. This may be explained by the more isotropic neutron exposure at the greater distances. Thus relatively more neutrons enter the phantom from the back and sides and thereby miss the plastic radiator in the NTA film that was carefully oriented for face-normal exposure.[6]

6. The estimate of the maximum local X and gamma-ray exposure

A comparison of Figs. 5 and 6 reveals that whereas the neutron dose inside the phantom is less than that on the outside front, the gamma dose is always greater inside than out. This may be due to a dose buildup, to n,γ reactions in the phantom water and in the emulsion, or to beta emission from the activated silver and bromine in the emulsion. Because it is impossible to separate these effects, and because the local photon energy spectrum is unknown, the precise total gamma exposure cannot be found from these data. However, since radium gamma rays give the least darkening of photographic film per roentgen exposure, the comparison of the experimental NTA films with calibration NTA films exposed to radium rays in air gives the maximum local gamma exposures. These are presented in Table 9. When it is scaled down to 10^{16} fissions, the gamma exposure at 200 m from a U-235 bomb is estimated as one-quarter of our maximum value.[7]

7. Attenuation of neutron and gamma dose by air

The SPRF measurements were taken at an elevation of 5000 ft where the air pressure was 0.82 atm. Figure 5 reveals that the fast-neutron attenuation in air is exponential in the first 200 m with λ = 225 m. This may be

compared with λ = 210 m for U-235 bomb neutrons at distances greater than 200 m.[8] The gamma exposure data of Fig. 6 give no evidence of an attenuation in air for the first 200 m. For much greater distances λ equals approximately 400 m for U-235-bomb gamma ray attenuation at 0.85 atm.[9]

V. SUMMARY

Nuclear track emulsion has been tested as a fast-neutron dosimeter by exposure of a human phantom to fission neutrons from a bare pulsed reactor. It was found that 600-μ-thick Ilford L.4 emulsion 2 cm on an edge yielded the absolute differential proton energy spectrum above 0.40 MeV and the average proton-track energy. From this the absolute differential local absorbed proton tissue dose, the local tissue thermal n,p dose, and the local fast-neutron energy spectrum at various positions in and around the phantoms were calculated.

The maximum and minimum total proton tissue doses around the phantom in rads per 10^{18} fissions were found to be 330 and 33 at 10 m, 45 and 5.9 at 25 m, 2.6 and 0.46 at 100 m, and 0.58 and 0.076 at 200 m. Independent estimates of the local proton tissue doses by use of NTA film generally agreed with these values.

The upper limits for the total local gamma exposures were obtained by a densitometer study of the 68 NTA films.

Graphs and tables of the local absolute differential proton tissue dose have been prepared for five locations in and around the phantoms at each of the five distances 10, 25, 50, 100, and 200 m from the reactor.

In addition to the reduced intensity attributable to the inverse square distance, the proton dose from neutrons was found to fall off exponetially between 10 and 200 m in air at 0.82 atm with γ = 225 m. However, there was

no evidence for an attenuation in air of the gamma rays over these distances.

A method is given to estimate the local fast-neutron energy spectrum. It is based on the slope of a smooth curve drawn through the corrected points of the proton recoil track energy spectrum that is measured in nuclear emulsion.

FOOTNOTE AND REFERENCES

* Work done under the auspices of the U. S. Atomic Energy Commission.

1 H. Akagi and R. L. Lehman, Neutron Dosimetry in and around Human Phantoms by use of Nuclear Track Emulsion, Health Phys. 9, 207-220 (1963).

2. P. D. O'Brien, Hazards Evaluation of the Sandia Pulsed Reactor Facility (SPRF), Sandia Corporation Report SC4357A (RR), Albuquerque, New Mexico, 1961 (unpublished).

3. J. L. Colp and P. D. O'Brien, The Sandia Pulsed Reactor Facility, Sandia Corporation Report SCR-229, Albuquerque, New Mexico, August 1960 (unpublished).

4. W. H. Buckalew, Neutron Flux and Spectra Measurements in the Sandia Pulsed Reactor Facility (SPRF), Sandia Corporation Report SCR-463, Albuquerque, New Mexico January 1962 (unpublished).

5. R. E. Peterson and G. A. Newby, An Unreflected U^{235} Critical Assembly, Nucl. Sci. Eng. 1, 112-125 (1956).

6. R. L. Lehman, Energy Response and Physical Properties of NTA Personnel Neutron Dosimeter Nuclear Track Film, Lawrence Radiation Laboratory Report UCRL-9513, January 13, 1961 (unpublished).

7. Samuel Glasstone, editor, The Effects of Nuclear Weapons, U. S. Atomic Energy Commission, Washington, D. C., April 1962, p. 410, Fig. 8.100.

8. Ibid., p. 411.

9. Ibid., p. 409.

Table 1. Burst-exposure data

Burst No.	Time	Date (Oct. 1961)	No. of Fissions $\times 10^{-16}$	Phantom No.	Distance from reactor (m)	Film packets[a]
1	1539	16	0.31	1	10	D-26 to D-30, D-1 to D-4, D-7
2	0845	17	1.48	1	25	D-36 to D-40, D-31 to D-35
3	1006	17	1.86	1	25	C-45 to C-49, C-40 to C-44
4	1150	17	1.86	1	50	D-41 to D-45, D-46 to D-50
5	1340	17	1.87	1	50	D-41 to D-45, D-46 to D-50
6	1550	17	1.97	1	50	C-50 to C-54, C-55 to C-57, C-59, C-58
All six	---	---	9.35	2	100	D-21 to D-25, D-9 to D-11, D-13, D-14
All six	---	---	9.35	3	200	D-5, D-6, D-8, D-12, D-20, D-16, D-15, D-17 to D-19

[a] In the same order as in Fig. 1.

Table 2. Energy spectra of protons in L.4 emulsions (10 m)

Channel No.	Energy (MeV)	D-26	D-27	D-28	D-29	D-30	D-1	D-2	D-3	D-4	D-7
1	0.030										
2	0.120										
3	0.225		72		36						
4	0.315	46	84	50	275	56				20	
5	0.395	129	728	56	237	150			19		44
6	0.47	197	409	457	465	286			10	167	121
7	0.535	242	661	460	863	588			251	282	573
8	0.600	513	1050	278	766	840			1086	1331	1048
9	0.665	502	1035	617	1292	1039			1484	1673	1928
10	0.72	455	796	797	965	1188			1741	1749	1956
11	0.78	504	950	664	497	751			1208	977	960
12	0.86	581	528	793	551	663			601	667	483
13	0.96	571	430	577	398	602			376	384	305
14	1.06	661	432	560	380	491			261	315	160
15	1.15	364	429	372	472	426			293	236	460
16	1.23	856	328	366	517	382			365	305	155
17	1.32	539	362	432	237	284			253	317	161
18	1.40	341	243	343	335	307			263	144	230
19	1.48	452	137	517	231	304			226	149	216
20	1.56	602	190	425	264	165			245	244	315
21	1.64	487	123	293	124	236			244	137	186
22	1.72	242	254	323	171	190			228	126	160
23	1.83	351	159	148	179	189			196	181	84
24	1.92	289	152	264	112	133			104	64	26
25	2.05	258	117	245	119	180			134	137	139
26	2.19	190	62	176	87	112			68	46	82
27	2.33	141	90	122	116	95			51	107	48
28	2.50	92	28	166	103	55			59	61	35
29	2.70	107	44	63	27	71			49	58	33
30	2.91	63	29	68	29	36			30	9	45
31	3.10	55	10	71	10	58			35	28	9
32	3.30	70	18	76	64	24			25	17	
33	3.50	21		34	29	20			11	9	
34	3.70	11		36	10	16			20	9	10
35	3.89	11		46	10				8		
36	4.09	22	10			16			8	9	
37	4.29	10	9	11		10					
38	4.49			12					12		
39	4.69			12		6			4		
40	4.90			12					8		
41	5.11								8		
42	5.31					6					
43	5.50			26							
44	5.69	12									
45	5.88			13		6					
46	6.08	12			11						
47	6.28					6					
48	6.49										
49	6.79										
50	7.19										

Table 3. Energy spectra of protons in L.4 emulsions (25 m)

Channel No.	Energy (MeV)	D-36	D-37	D-38	D-39	D-40	D-31	D-32	D-33	D-34	D-35
1	0.030										
2	0.120						6				
3	0.225			20	17	17	41		13		
4	0.315		24	46	260	101	88	108	46		
5	0.395	70	137	179	403	23	277	101	60	44	24
6	0.47	254	238	390	927	466	399	394	225	48	106
7	0.535	274	288	780	473	608	755	732	657	208	315
8	0.600	348	373	730	1113	840	1165	1749	1328	990	909
9	0.665	726	602	762	1395	1140	1703	1644	2146	1982	1486
10	0.72	475	667	832	851	1314	1357	1937	1893	2102	1224
11	0.78	586	762	785	657	849	948	842	974	834	851
12	0.86	542	912	668	569	622	590	336	425	611	690
13	0.96	659	605	605	530	465	443	200	303	304	298
14	1.06	654	459	512	377	325	358	193	228	266	430
15	1.15	504	476	467	372	412	215	284	236	368	385
16	1.23	550	524	379	391	256	281	158	241	193	298
17	1.32	656	471	348	203	388	186	182	109	301	442
18	1.40	352	283	193	127	361	160	228	114	84	437
19	1.48	522	505	224	218	329	209	196	143	86	214
20	1.56	520	498	233	136	91	118	61	79	292	272
21	1.64	513	401	321	117	189	103	105	117	255	332
22	1.72	270	276	221	97	326	103	87	100	176	247
23	1.83	282	268	193	203	136	94	30	72	134	166
24	1.92	247	241	196	106	106	111	59	102	91	129
25	2.05	233	171	144	70	155	61	101	75	97	122
26	2.19	147	143	161	118	95	61	85	72	81	115
27	2.33	114	104	125	73	61	54	44	47	60	53
28	2.50	120	162	91	62	54	21	32	51	79	58
29	2.70	106	72	67	25	26	27		33	58	92
30	2.91	76	44	73	46	55	11	33	32	36	40
31	3.10	49	69	54	19	76	19	17	22	19	52
32	3.30	54	53	40		35	3	8	3	52	57
33	3.50	19	55	21	18		4	24	10	36	30
34	3.70	20	24	66	10	10	8		7	19	11
35	3.89	10			9	19			7	18	10
36	4.09	20	12	22		10			4	10	42
37	4.29	9	11	20		9	4		3	18	10
38	4.49		11	11	9				4		10
39	4.69	10							4		11
40	4.90					9					
41	5.11		23							9	10
42	5.31						4		4		11
43	5.50										
44	5.67		13								
45	5.88										
46	6.08										
47	6.28										
48	6.49										
49	6.79										
50	7.19										

Table 4. Energy spectra of protons in L.4 emulsions (25 m, Cadmium)

Channel No.	Energy (MeV)	C-45	C-46	C-47	C-48	C-49	C-40	C-41	C-42	C-43	C-44
1	0.030										
2	0.120										
3	0.225	20	17		18	17					8
4	0.315	69	302		206	101					59
5	0.395	181	270		231	226					244
6	0.47	366	564		603	466					386
7	0.535	515	846		460	688					364
8	0.600	385	923		716	896					536
9	0.665	536	701		1196	614					617
10	0.72	665	550		907	825					766
11	0.78	901	755		772	786					773
12	0.86	694	654		502	654					603
13	0.96	651	757		546	654					524
14	1.06	455	451		425	505					603
15	1.15	622	505		440	505					606
16	1.23	473	393		443	236					425
17	1.32	515	388		502	450					482
18	1.40	414	234		391	255					334
19	1.48	452	285		269	351					388
20	1.56	340	160		280	320					303
21	1.64	406	260		217	260					302
22	1.72	205	309		83	228					336
23	1.83	97	255		104	221					217
24	1.92	259	66		122	226					215
25	2.05	178	70		115	141					159
26	2.19	109	47		73	83					198
27	2.33	127	86		63	37					163
28	2.50	61	54		82	36					79
29	2.70	88	42		52	26					50
30	2.91	42			47	37					36
31	3.10	22	10		49	38					75
32	3.30	30	9		18	44					21
33	3.50	10				27					4
34	3.70	11	10		10	10					29
35	3.89	11	19								5
36	4.09	22			10						14
37	4.29				9	9					4
38	4.49										9
39	4.69	11	10								5
40	4.90				10						9
41	5.11				10						
42	5.31	12									5
43	5.50				11						
44	5.67					11					
45	5.88										
46	6.08										
47	6.28					10					
48	6.49										
49	6.79										3
50	7.19										

Table 5. Energy spectra of protons in L.4 emulsions (50 m, Cadmium)

Channel No.	Energy (MeV)	C-50	C-51	C-52	C-53	C-54	C-55	C-56	D-48	C-59	C-58
1	0.0300										
2	0.1200										
3	0.225		18					19	7		
4	0.315		188					156	25		
5	0.395		305					200	56		
6	0.47		766					299	163		
7	0.535		606					732	385		
8	0.600		728					837	1362		
9	0.665		791					647	2005		
10	0.72		668					778	1817		
11	0.78		851					488	981		
12	0.86		681					706	537		
13	0.96		609					667	265		
14	1.06		338					560	255		
15	1.15		565					559	210		
16	1.23		327					457	204		
17	1.32		234					272	195		
18	1.40		265					588	212		
19	1.48		274					437	128		
20	1.56		238					228	161		
21	1.64		393					131	128		
22	1.72		305					216	108		
23	1.83		195					113	141		
24	1.92		193					338	127		
25	2.05		103					109	76		
26	2.19		99					39	89		
27	2.33		51					95	82		
28	2.50		28					99	70		
29	2.70		18					56	25		
30	2.91		38					10	38		
31	3.10		40					11	16		
32	3.30		18					29	25		
33	3.50							20	4		
34	3.70		20					43	4		
35	3.89								15		
36	4.09							32	8		
37	4.29								4		
38	4.49		10						12		
39	4.69								4		
40	4.90										
41	5.11		10								
42	5.31										
43	5.50										
44	5.69										
45	5.88										
46	6.08										
47	6.28										
48	6.49										
49	6.79										
50	7.19										

Table 6. Energy spectra of protons in L.4 emulsions (100 m)

Channel No.	Energy (MeV)	D-21	D-22	D-23	D-24	D-25	D-9	D-10	D-11	D-13	D-14
1	0.030										
2	0.120										
3	0.225		34	19					7		
4	0.315		159	108		176	25		23	35	
5	0.395	69	334	413	89	197	92		79	116	
6	0.47	251	678	423	194	263	160	150	162	127	129
7	0.535	433	731	940	340	772	335	216	492	523	500
8	0.6000	975	995	815	719	1199	938	1001	1389	1540	1500
9	0.665	1018	1038	850	1502	1962	1708	1643	2027	2337	2057
10	0.72	1314	995	626	996	1368	1536	2030	1753	2575	1830
11	0.78	676	652	780	1150	857	1170	1382	1048	838	793
12	0.86	771	614	405	501	621	562	485	475	295	395
13	0.96	616	526	408	527	402	457	316	280	104	253
14	1.06	536	481	661	464	263	361	314	308	171	341
15	1.15	345	369	383	591	255	183	191	275	129	196
16	1.23	362	330	381	486	325	281	342	221	152	289
17	1.32	335	303	308	323	179	267	292	182	123	215
18	1.40	218	336	275	273	227	261	195	173	73	89
19	1.48	292	151	236	390	149	296	67	127	94	138
20	1.56	210	113	246	68	133	187	210	195	79	240
21	1.64	169	47	229	140	115	145	145	91	122	174
22	1.72	233	241	70	225	111	160	150	114	98	120
23	1.83	157	201	256	185	83	153	87	112	102	107
24	1.92	217	236	186	118	52	114	163	51	68	112
25	2.05	159	69	137	195	55	144	86	71	36	118
26	2.19	121	70	191	164	35	82	73	73	61	100
27	2.33	151	61	146	85	84	65	88	52	32	64
28	2.50	119	53	115	71	17	73	46	59	54	66
29	2.70	61	34	64	25		59	78	30	29	9
30	2.91	19	9	30	27	9	34	19	21	16	39
31	3.10	39	19	72	28	9	43	39	15	8	50
32	3.30	18	17	38	35	17	18	9	17	15	18
33	3.50	9	45	10	36	18	22	9	7	16	19
34	3.70	10		32		10	20	10	15	8	
35	3.89		9	30	37	9	8	38	4		19
36	4.09	10	10		10	9	16	10	4	8	
37	4.29	9		29			4	9	3	8	
38	4.49	19		10			8		4	8	
39	4.69		10	21		19	4	10			10
40	4.90	10			9						
41	5.11	20					4		7		
42	5.31		10	33			4		8		
43	5.50			23							
44	5.69							11			
45	5.88										
46	6.08	11									
47	6.28										
48	6.49										
49	6.79										
50	7.19										

Table 7. Energy spectra of protons in L.4 emulsions (200 m)

Channel No.	Energy (MeV)	D-5	D-6	D-8	D-12	D-20	D-16	D-15	D-17	D-18	D-19
1	0.030										
2	0.120										
3	0.225	18	18	34					14		
4	0.315	62	42	39	73	22	17		58		
5	0.395	69	190	263	327	24	93		93		
6	0.47	251	516	429	312	212	132	25	233	93	90
7	0.535	514	667	462	552	257	284	293	317	225	195
8	0.600	803	1030	1088	1220	1118	1147	734	1192	1295	824
9	0.665	1556	1536	1164	2122	1546	2032	2180	2090	2594	1909
10	0.72	1064	1125	1098	1304	1682	1644	2033	1554	2106	2474
11	0.78	1095	761	703	799	1188	1132	1205	1235	1425	2025
12	0.86	586	516	667	431	583	677	495	582	448	572
13	0.96	546	416	418	312	520	320	243	313	195	190
14	1.06	185	398	245	246	351	321	255	201	187	149
15	1.15	249	472	309	255	343	325	302	217	177	172
16	1.23	503	289	363	303	212	334	377	163	278	90
17	1.32	314	236	318	186	177	304	185	211	58	188
18	1.40	370	223	124	270	161	211	129	228	100	98
19	1.48	247	231	341	299	237	127	221	199	83	101
20	1.56	281	192	244	249	296	161	92	104	129	210
21	1.64	338	124	298	129	102	137	214	156	89	109
22	1.72	100	171	221	148	176	61	164	94	77	90
23	1.83	226	179	132	77	128	98	188	91	32	63
24	1.92	122	140	245	60	158	82	80	110	38	85
25	2.05	144	118	68	102	91	93	156	82	0	104
26	2.19	61	100	115	43	89	59	84	54	78	54
27	2.33	50	52	95	56	66	30	62	66	58	34
28	2.50	82	66	78	40	87	33	54	37	17	57
29	2.70	26	63	41	31	28	28	26	46	64	39
30	2.91	28	10	62	8	59	30	28	19	17	25
31	3.10	10	60	65	9	21	8	38	47	9	18
32	3.30	18	18	59		9	18	26	14	25	8
33	3.50		19	9	17	0	11	37	53	9	8
34	3.70	10		9	9	11	12	20	20	9	
35	3.89			27		10	4	19	27	0	
36	4.09	10		38		10			8	0	
37	4.29			26			4	9	7	17	
38	4.49			54			4		12	18	
39	4.69		10	10			4	10	8	9	
40	4.90			9			4		0	9	
41	5.11			9					0	0	
42	5.31							10	8	0	19
43	5.50								4		
44	5.69		11						4		
45	5.88						4			10	
46	6.08										
47	6.28										
48	6.49								4	10	
49	6.79			5			5			5	
50	7.19								2		

Table 8. Proton track data from L.4 emulsions exposed to SPR bursts

Distance (m)	Emulsion No.	Neutron exposure fissions ($\times 10^{16}$)	Measured track density [t/cm^3 ($\times 10^{-6}$)]	Tracks lost 0-0.66 MeV(%)	Correct track density [t/cm^3 ($\times 10^{-6}$)]	Correct density per fission ($\times 10^{9}$)	Correct average proton track energy (MeV)	Emulsion proton dose (ergs/cm^3-fission ($\times 10^{16}$)	Thermal n, p tracks (%)	Thermal n, p emulsion dose [ergs/cm^3-fission ($\times 10^{16}$)]	Proton recoil emulsion dose [ergs/cm^3-fission ($\times 10^{16}$)]
10	D-26	0.312	18.7[a]	45	34.0	10.9	1.03	179.6	1.03	1.1	179.0
	D-27	0.312	21.0	52	42.5	13.7	0.80	171.0	11.8	13.2	158.0
	D-28	0.312	16.0	48	31.0	9.4	0.80	120.0	0	0	120.0
	D-29	0.312	3.75	54	8.2	2.6	0.72	30.0	10.0	2.5	27.5
	D-30	0.312	2.5	47	4.7	1.50	0.79	18.5	10.0	1.4	17.1
	D-1	0.312	[b]								
	D-2	0.312	[b]								
	D-3	0.312	9.0	37	14.3	4.6	0.87	64.0	25.1	11.1	52.7
	D-4	0.312	3.8[a]	40	6.3	2.0	0.80	26.0	28.0	5.4	20.5
	D-7	0.312	8.8	46	16.3	5.2	0.67	56.0	18.5	9.3	46.3
25	D-36	1.47	13.2	40	22.0	1.50	1.00	24.0	2.3	0.33	23.7
	D-37	1.47	13.5	34	20.5	1.40	1.08	24.0	6.3	0.84	23.1
	D-38	1.47	13.3	37	21.0	1.43	0.80	18.9	6.0	0.80	18.3
	D-39	1.47	2.4	50	4.8	0.325	0.70	3.65	11.0	0.35	3.30
	D-40	1.47	1.95	50	3.9	0.27	0.83	3.50	13.4	0.47	3.05
	D-31	1.47	16.0	50	32.0	2.18	0.74	25.0	22.5	5.60	19.4
	D-32	1.47	8.8	52	18.3	1.25	0.66	13.1	26.0	3.20	10.0
	D-33	1.47	5.6	48	10.8	0.735	0.71	8.35	31.0	2.60	5.75
	D-34	1.47	2.4	51	4.9	0.335	0.73	3.90	17.0	0.60	3.30
	D-35	1.47	4.9[a]	47	9.3	0.63	0.75	7.6	14.0	0.84	6.70
25	C-45	1.86	17.0	44	30.4	1.63	0.92	24.0	2.0	0.31	23.7
	C-46	1.86	14.6	51	30.0	1.60	0.74	18.9	7.1	1.10	17.8
	C-47[c]	1.86									
	C-48	1.86	2.8	47	5.3	0.29	0.80	3.7	12.6	0.35	3.3
	C-49	1.86	2.35	51	4.8	0.26	0.79	3.2	4.2	0.10	3.1
	C-44[c]	1.86	4.0	43	7.0	0.38	0.94	5.6	0	0	5.6
50[d]	D-48	3.74	3.3	38	5.3	0.14	0.80	1.82	38.0	0.52	1.3
	C-51	1.98	5.2	44	9.3	0.47	0.84	6.3	0	0	6.3
	C-56	1.98	2.1	44	3.7	0.19	0.87	2.7	6.7	0.18	2.5
100	D-21	9.4	5.45	48	10.5	0.11	0.82	1.46	8.0	0.082	1.40
	D-22	9.4	6.35	51	12.9	0.14	0.72	1.59	9.1	0.12	1.50
	D-23	9.4	4.60	49	9.2	0.100	0.84	1.32	7.3	0.07	1.25
	D-24	9.4	1.63	44	2.9	0.031	0.83	0.41	13.5	0.04	0.37
	D-25	9.4	2.25	52	4.7	0.0505	0.68	0.54	27.5	0.15	0.39
	D-9	9.4	4.7	44	8.4	0.089	0.80	1.14	21.8	0.19	0.96
	D-10	9.4	3.3	48	6.3	0.068	0.74	0.80	18.8	0.12	0.68
	D-11	9.4	2.4	43	4.2	0.0445	0.77	0.55	35.0	0.19	0.36
	D-13	9.4	1.75	38.5	2.8	0.030	0.78	0.38	44.0	0.17	0.21
	D-14	9.4	1.9	47	3.6	0.038	0.72	0.44	15.0	0.055	0.39
200	D-5	9.4	1.44	43	2.52	0.268	0.81	0.35	12.3	0.042	0.302
	D-6	9.4	1.47	42	2.53	0.027	0.80	0.34	18.5	0.048	0.300
	D-8	9.4	1.06	47	2.00	0.0215	0.80	0.27	11.8	0.030	0.245
	D-12	9.4	0.70	33	1.05	0.011	0.75	0.13	13.6	0.015	0.120
	D-20	9.4	0.40	47	0.755	0.0080	0.77	0.10	15.4	0.012	0.087
	D-16	9.4	1.07	41	1.82	0.0189	0.77	0.235	37.0	0.068	0.170
	D-15	9.4	0.71	37	1.13	0.0120	0.78	0.15	20.0	0.023	0.130
	D-17	9.4	0.38	40	0.63	0.0067	0.80	0.086	28.0	0.018	0.068
	D-18	9.4	0.31	32	0.455	0.0049	0.766	0.059	50.0	0.023	0.036
	D-19	9.4	0.62	27	0.85	0.0090	0.79	0.11	41.2	0.036	0.079

[a] Estimate from NTA film

[b] Film opaque from gamma rays

[c] C-40 to C-43, C-47 not scanned

[d] Only those listed were scanned

Table 9. Proton tissue dose from irradiation by SPR bursts

Distance (m)	Emulsion No.	Proton-recoil tissue dose [rads/fission($\times 10^{18}$)]	N(n, p)C tissue dose [rads/fission($\times 10^{18}$)]	Total proton tissue dose [rads/fission($\times 10^{18}$)]	% N(n, p)C dose	NTA tracks/field-fission($\times 10^{16}$)	Tissue dose based on NTA[a] [rems/fission($\times 10^{16}$)]	Ratio NTA dose est. / Ilford dose	Air equivalent exposure total γ rays [roentgens/fission($\times 10^{16}$)]
10	D-26	332	0.45	333	(0)	230	34.6	1.04	1.5
	D-27	295	5.0	300	2	210	31.0	1.05	1.4
	D-28	220	(0)	220	(0)	160	23.9	1.07	0.9
	D-29	51	1.0	52	2	33	4.9	0.94	0.5
	D-30	32	0.6	33	2	21	3.1	0.94	0.4
	D-1	[b](220 est.)				165	25.0		2.6
	D-2	[b](150 est.)				110	16.7		2.7
	D-3	98.5	4.5	103	4	63	9.55	0.94	2.0
	D-4	38	2.0	40	5	27	4.05	1.01	1.25
	D-7	86.7	3.8	90.5	4	75	11.3	1.25	2.10
25	D-36	44.3	0.1	44.4	0	35	5.25	1.19	0.20
	D-37	43.3	0.3	43.6	1.0	32	4.8	1.10	0.18
	D-38	31	0.4	31.4	1.0	24	3.58	1.13	0.12
	D-39	6.15	0.14	6.3	2.0	4.1	0.6	0.94	0.09
	D-40	5.65	0.19	5.85	2.0	3.3	0.48	0.83	0.07
	D-31	37.0	2.2	39.0	5.5	(24)	(3.58)	(0.98)	(0.33 est.)
	D-32	18.7	1.3	20.0	6.5	16.0	2.4	1.19	0.35
	D-33	10.7	1.0	11.7	8.5	9.4	1.43	1.19	0.27
	D-34	6.2	0.3	6.5	4.5	4.1	0.6	0.92	0.17
	D-35	12.6	0.3	12.9	2.5	8.9	1.3	1.01	0.29
25	C-45	44.3	0.1	44.4	(0)	29.0	4.30	0.96	0.25
	C-46	33.4	0.4	33.9	1	27.0	4.05	1.19	0.27
	C-47	[c]		(25 est.)		19.0	2.85		0.18
	C-48	6.2	0.14	6.4	2	3.8	0.60	0.93	0.10
	C-49	5.9	0.04	5.9	1	3.2	0.50	0.81	0.07
25	C-40	[c]		(28 est.)		22.0	3.30	1.19	0.37
	C-41	[c]		(18 est.)		12.0	1.80	0.99	0.37
	C-42	[c]		(9.0 est.)		6.9	1.01	1.12	0.25
	C-43	[c]		(5.0 est.)		3.5	0.53	1.05	0.17
	C-44	10.6	0	10.6	0	7.9	1.19	1.12	0.29
50	D-41	[c]		(13 est.)		7.0	1.07		0.052
	D-42	[c]		(13 est.)		7.0	1.07		0.052
	D-43	[c]		(8.8 est.)		4.8	0.72		0.043
	D-44	[c]		(1.7 est.)		0.95	0.14		0.026
	D-45	[c]		(1.6 est.)		0.85	0.13		0.025
	D-46	[c]		(9.6 est.)		5.3	0.79		0.092
	D-47	[c]		(6.6 est.)		3.6	0.54		0.096
	D-48	2.43	0.21	2.64	8	1.4	0.22	0.81	0.070
	D-49	[c]		(1.45 est.)		0.82	0.12		0.050
	D-50	[c]		(3.2 est.)		1.8	0.27		0.075
50	C-50	[c]		(13 est.)		7.0	0.11		0.065
	C-51	11.7	0	11.7	0	6.5	0.95	0.81	0.065
	C-52	[c]		(7.8 est.)		4.5	0.66		0.053
	C-53	[c]		(1.6 est.)		0.91	0.13		0.038
	C-54	[c]		(1.6 est.)		0.88	0.13		0.039
	C-55	[c]		(8.6 est.)		4.7	0.7		0.096
	C-56	4.65	0.07	4.7	1.5	3.0	0.45	0.94	0.092
	C-57	2.4	0.01	2.4	0	1.3	0.19	0.80	0.064
	C-59	[c]		(4.4 est.)		0.78	0.12		0.048
	C-58	[c]		(2.7 est.)		1.5	0.23		0.065
100	D-21	2.6	0.03	2.6	1	1.30	0.19	0.74	0.017
	D-22	2.75	0.05	2.8	2	1.40	0.20	0.73	0.015
	D-23	2.3	0.03	2.3	1.5	1.20	0.18	0.77	0.012
	D-24	0.69	0.02	0.71	3	0.29	0.042	0.60	0.0075
	D-25	0.73	0.06	0.79	5	0.25	0.037	0.48	0.007
	D-9	1.79	0.08	1.87	4	1.20	0.18	0.95	0.027
	D-10	1.27	0.05	1.32	4	0.70	0.11	0.81	0.023
	D-11	0.67	0.076	0.75	10	0.41	0.06	0.80	0.019
	D-13	0.39	0.07	0.46	14.5	0.22	0.033	0.73	0.014
	D-14	0.73	0.02	0.75	2.5	0.41	0.06	0.80	0.02
200	D-5	0.56	0.016	0.576	3	0.26	0.039	0.70	0.0032
	D-6	0.55	0.02	0.57	3	0.28	0.042	0.74	0.0032
	D-8	0.46	0.01	0.47	1.5	0.21	0.031	0.66	0.0032
	D-12	0.22	0.006	0.23	2.5	0.061	0.009	0.39	0.0024
	D-20	0.16	0.005	0.17	3	0.054	0.008	0.49	0.0024
	D-16	0.435	0.028	0.46	6	0.18	0.026	0.60	0.0056
	D-15	0.24	0.009	0.25	3.5	0.09	0.013	0.53	0.0053
	D-17	0.125	0.007	0.135	5	0.059	0.009	0.66	0.0035
	D-18	0.067	0.0093	0.076	12	0.042	0.006	0.79	0.0031
	D-19	0.15	0.014	0.16	9	0.09	0.013	0.83	0.0043

[a] Based on 6.7 tracks per field per rem for mock-fission neutron source in air.[6]

[b] Estimated: too dark to scan

[c] Not scanned

Table 10. Proton tissue dose from irradiation by pulsed-reactor neutrons

Distance (m)	Emulsion	Dose (%) by protons of energy interval (in MeV): 0 - 0.5	0.5 - 1.0	1.0 - 1.5	1.5 - 2.0	2.0 - 2.5	2.5 - 3.0	3.0 - 4.0	4.0 - 5.0	5.0 - 7.0	Total dose [rads/fission($\times 10^{18}$)]
10	D-26	9.5	15.5	23.0	20.0	11.5	7.5	9.0	3.0	1.0	335
	D-3	16.5	25.0	17.5	14.0	9.0	5.5	7.0	3.0	2.5	105
	D-4	17.0	27.5	19.0	13.5	8.5	5.5	8.0	1.0	0	40
	D-30	18.0	26.5	20.0	14.0	9.0	5.5	5.5	1.5	0	33
25	D-36	12.0	18.5	21.5	18.0	12.0	8.0	7.5	2.0	0.5	44.5
	D-31	18.5	31.5	18.0	12.0	8.5	5.0	4.5	1.5	0.5	39.0
	D-33	17.0	30.0	16.0	11.0	9.0	6.5	6.5	2.5	1.5	11.5
	D-34	17.0	28.0	15.0	11.5	9.0	7.0	9.0	3.0	0.5	6.5
	D-40	18.0	24.0	18.0	13.5	9.5	6.5	7.0	2.5	1.0	5.85
50	C-51	18.5	26.0	20.5	14.0	8.5	5.0	5.0	1.5	1.0	11.5
	C-56	15.0	25.0	21.0	15.0	9.5	6.5	6.0	1.5	0.5	4.7
	D-48	14.0	29.0	15.0	13.0	10.0	6.5	7.5	3.0	2.0	2.65
100	D-21	17.0	25.0	18.0	13.5	10.0	7.0	6.5	2.0	1.0	2.6
	D-9	16.0	26.5	15.5	15.0	9.5	6.0	7.0	3.0	1.5	1.85
	D-11	17.5	30.0	18.0	12.0	8.0	5.0	5.5	2.5	1.5	0.75
	D-13	16.0	27.5	15.5	13.0	9.5	6.5	7.0	3.5	1.5	0.46
	D-25	21.5	39.0	15.5	9.0	5.0	3.0	3.5	2.0	1.5	0.79
200	D-5	18.5	27.0	20.0	14.5	9.0	5.0	4.0	1.5	0.5	0.575
	D-16	15.5	30.0	18.0	13.0	8.0	5.0	6.0	2.5	2.0	0.46
	D-17	16.0	27.5	14.5	12.0	8.5	6.0	8.0	5.0	2.5	0.135
	D-18	19.0	37.5	15.0	9.0	6.0	4.5	6.0	3.0	0	0.076
	D-20	17.5	28.0	17.0	13.5	10.0	6.5	5.5	1.5	0.5	0.17

FIGURE CAPTIONS

Fig. 1. Cross section of phantom at center plane, showing orientation of the 10 film packets.

Fig. 2. Proton spectrum from Ilford film D-16 and derived spectra.

Fig. 3. Proton recoil and proton recoil dose spectra based upon the pure U-235 fission neutron spectrum.

Fig. 4. Background track distribution in Ilford films.

Fig. 5. Response of NTA films.

Fig. 6. Relative optical density of NTA films.

Fig. 7. Absolute differential tissue dose at 10 m.

Fig. 8. Absolute differential tissue dose at 25 m.

Fig. 9. Absolute differential tissue dose at 50 m.

Fig. 10. Absolute differential tissue dose at 100 m.

Fig. 11. Absolute differential tissue dose at 200 m.

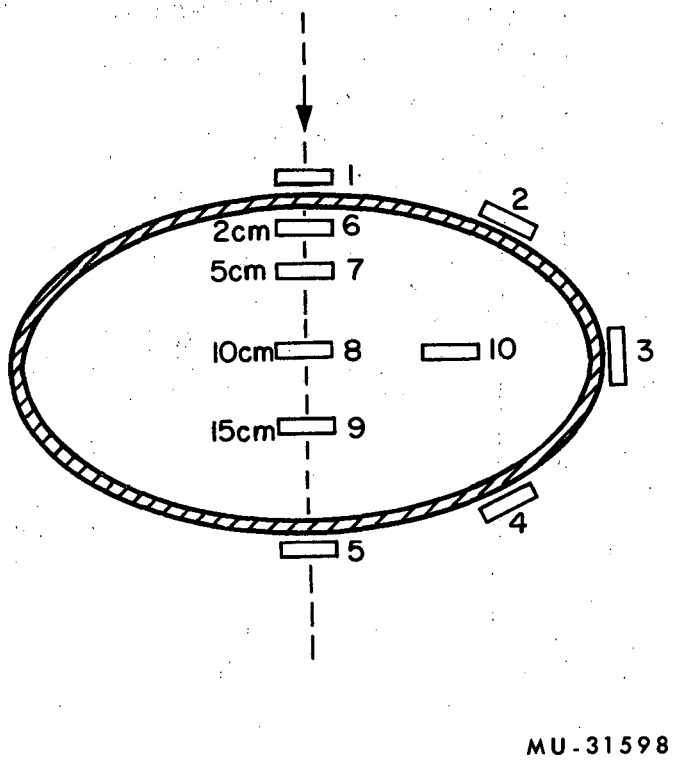

Fig. 1

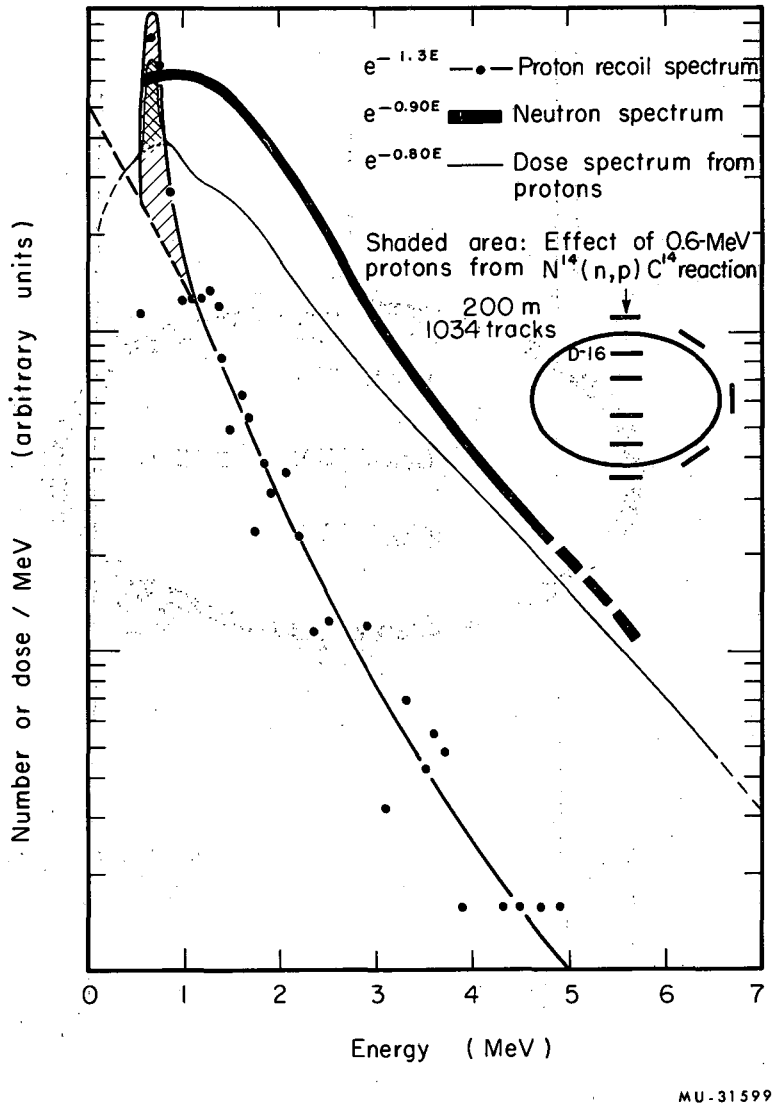
$e^{-1.3E}$ Proton recoil spectrum
$e^{-0.90E}$ Neutron spectrum
$e^{-0.80E}$ Dose spectrum from protons
Shaded area: Effect of 0.6-MeV protons from $N^{14}(n,p)C^{14}$ reaction
200 m
1034 tracks
D-16
Number or dose / MeV (arbitrary units)
0
1
2
3
4
5
6
7
Energy (MeV)
MU-31599

Fig. 2

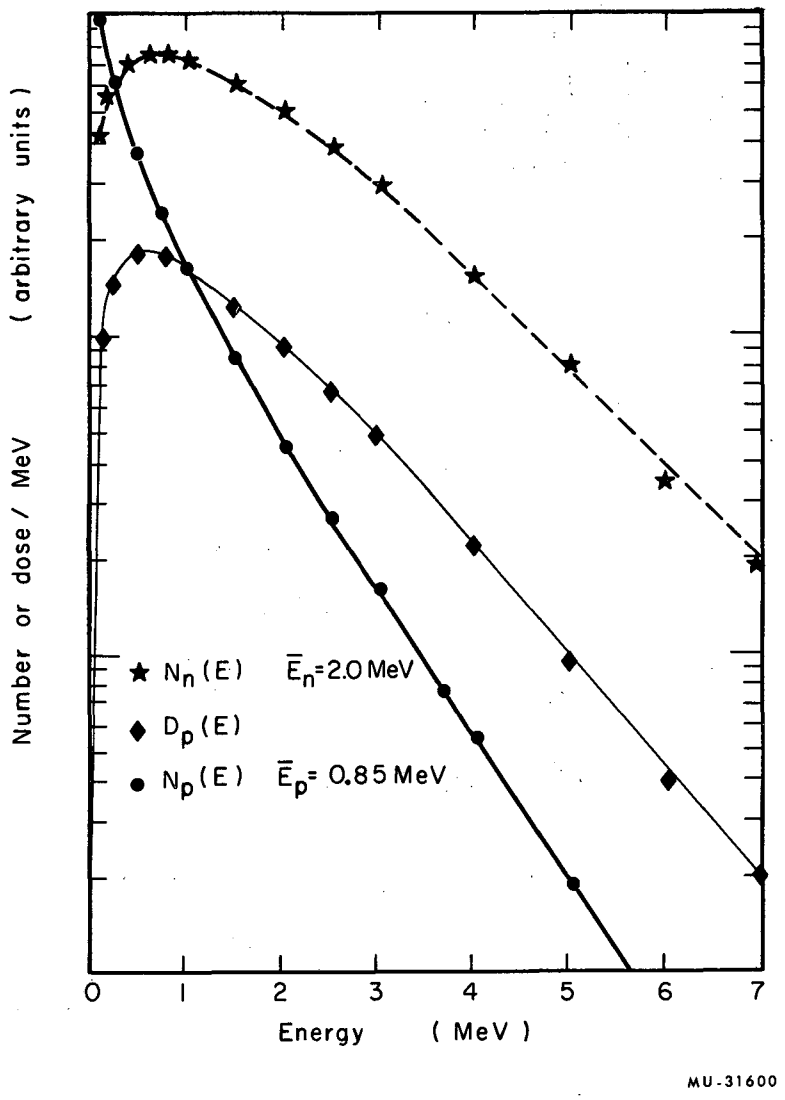
Number or dose / MeV (arbitrary units)
Energy (MeV)
0
1
2
3
4
5
6
7
$N_n(E)$ $\bar{E}_n$=2.0 MeV
$D_p(E)$
$N_p(E)$ $\bar{E}_p$= 0.85 MeV
MU-31600

Fig. 3

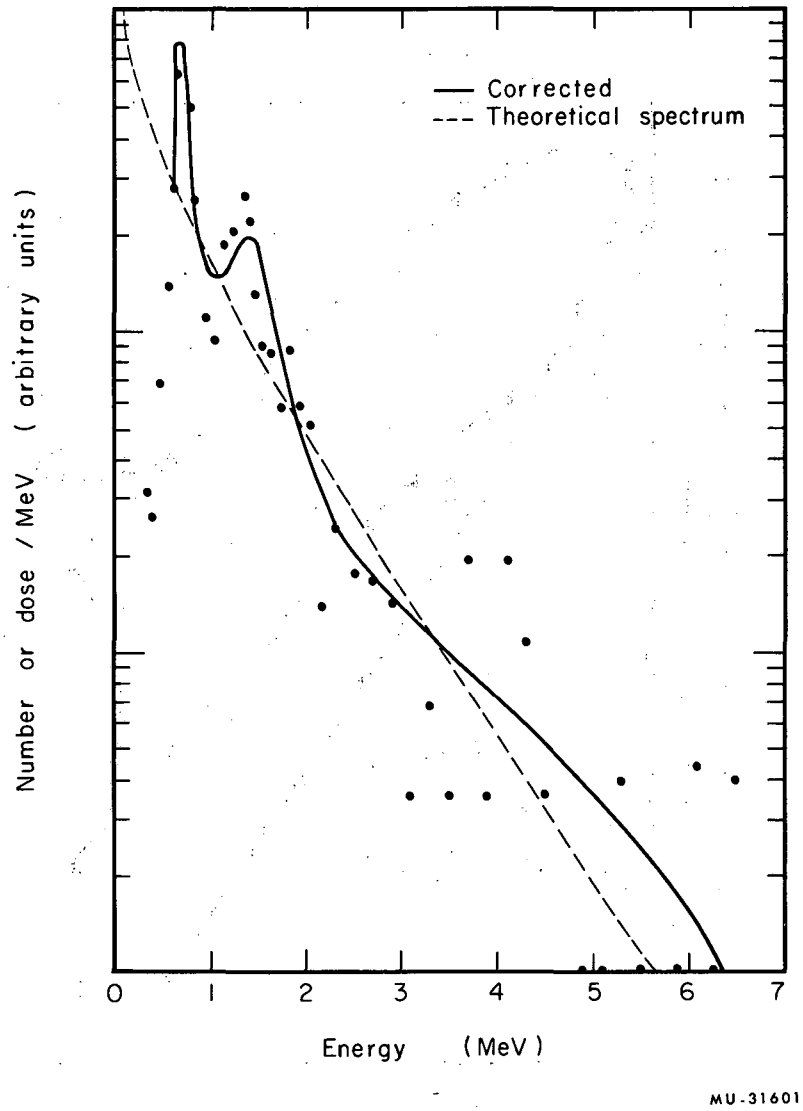
Corrected
Theoretical spectrum
Number or dose / MeV (arbitrary units)
0
1
2
3
4
5
6
7
Energy (MeV)
MU-31601

Fig. 4

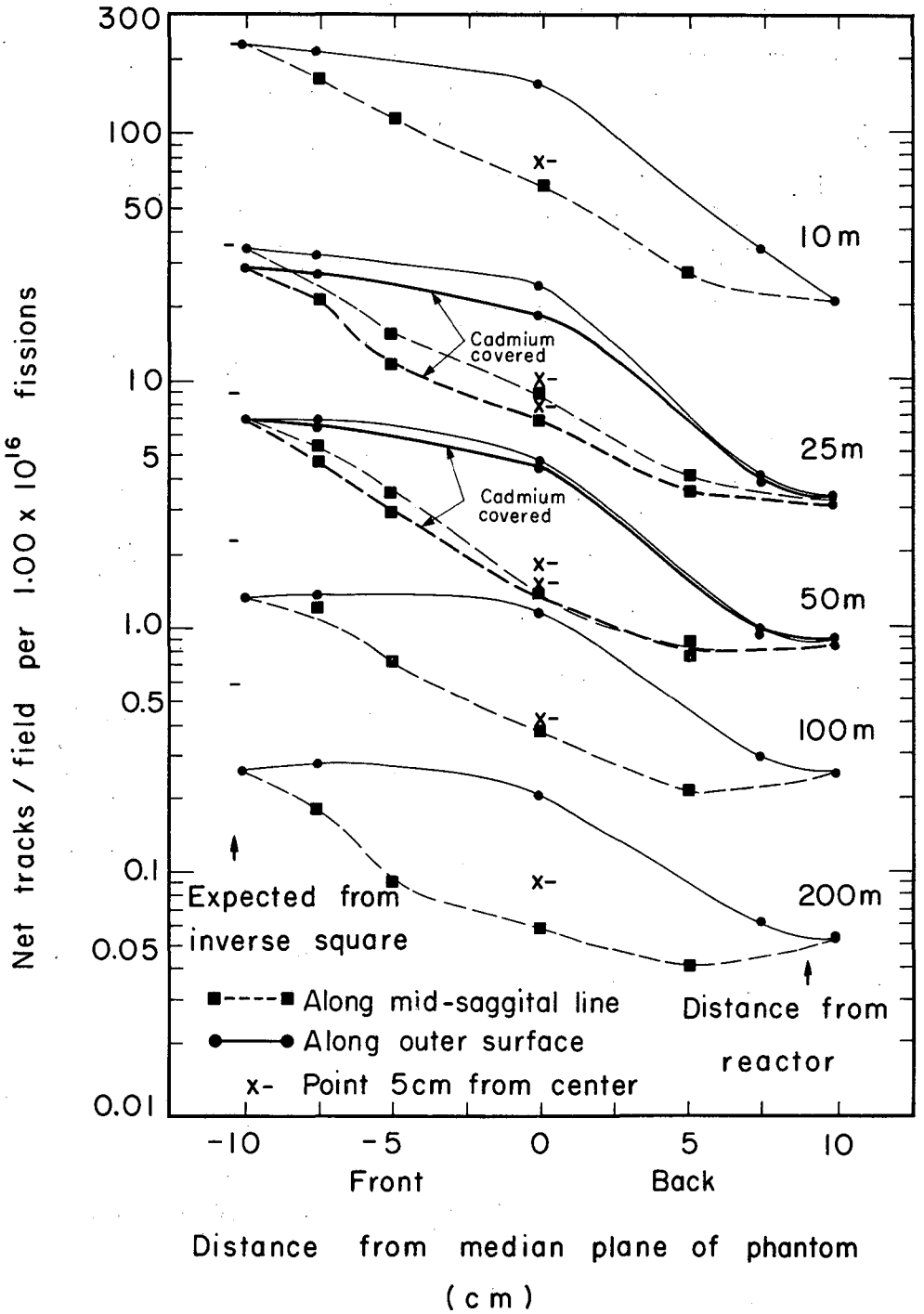

MUB-2022

Fig. 5

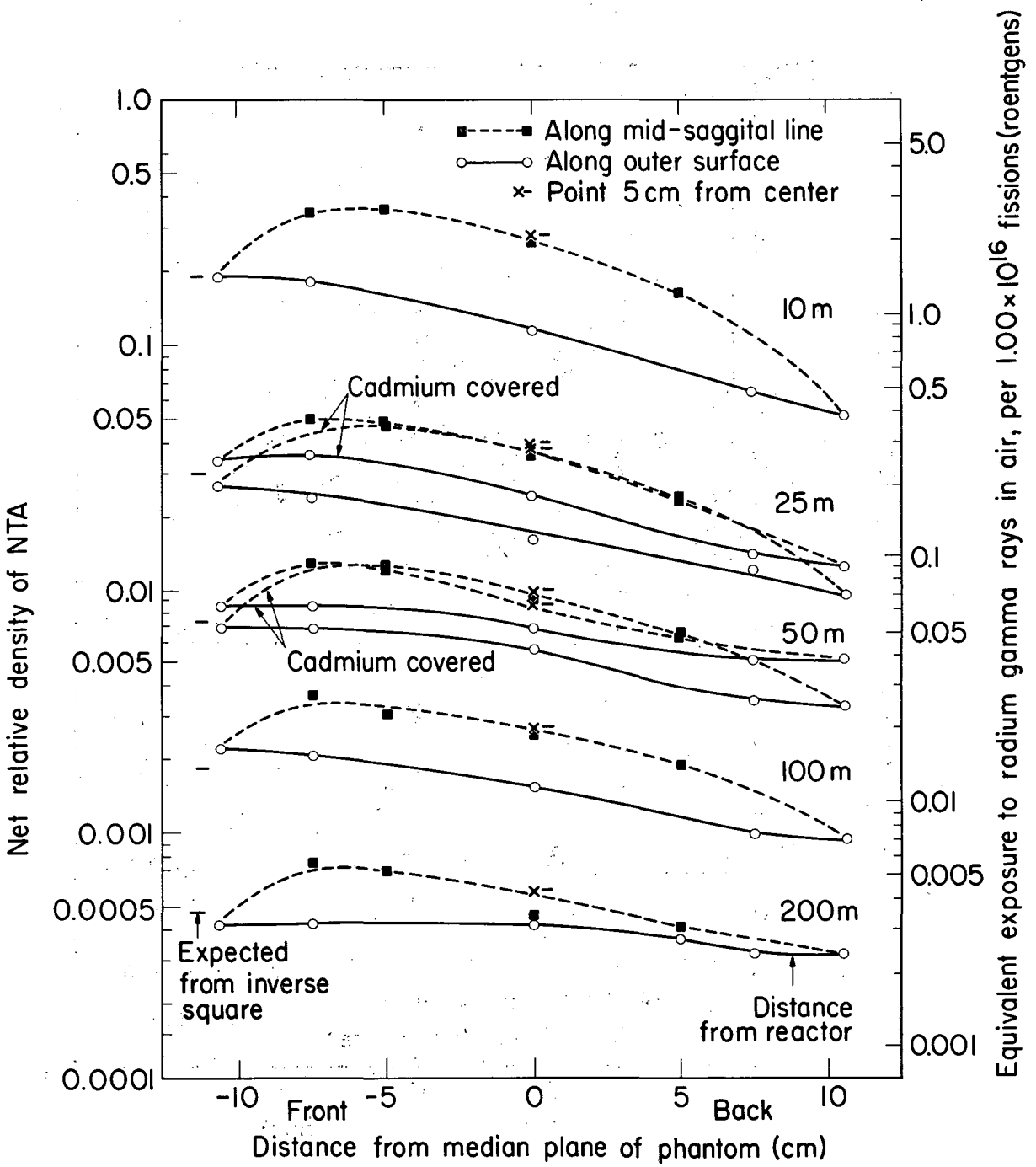
Along mid-saggital line
Along outer surface
Point 5 cm from center
10 m
25 m
50 m
100 m
200 m
Cadmium covered
Cadmium covered
Expected from inverse square
Distance from reactor
Front
Back
Distance from median plane of phantom (cm)
Net relative density of NTA
Equivalent exposure to radium gamma rays in air, per 1.00×10^16 fissions (roentgens)
1.0
0.5
0.1
0.05
0.01
0.005
0.001
0.0005
0.0001
5.0
1.0
0.5
0.1
0.05
0.01
0.005
0.001
-10
-5
0
5
10
MUB-2023

Fig. 6

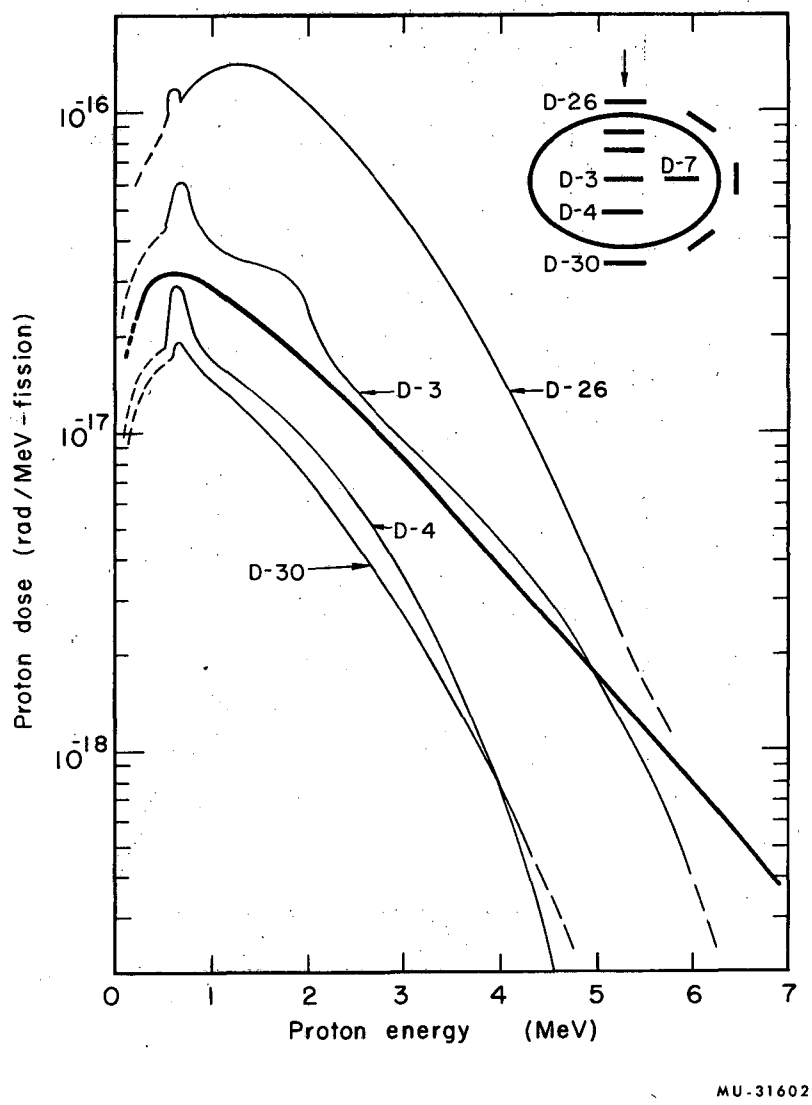
D-26
D-7
D-3
D-4
D-30
D-3
D-26
D-4
D-30
10^{-16}
10^{-17}
10^{-18}
Proton dose (rad/MeV-fission)
0
1
2
3
4
5
6
7
Proton energy (MeV)
MU-31602

Fig. 7

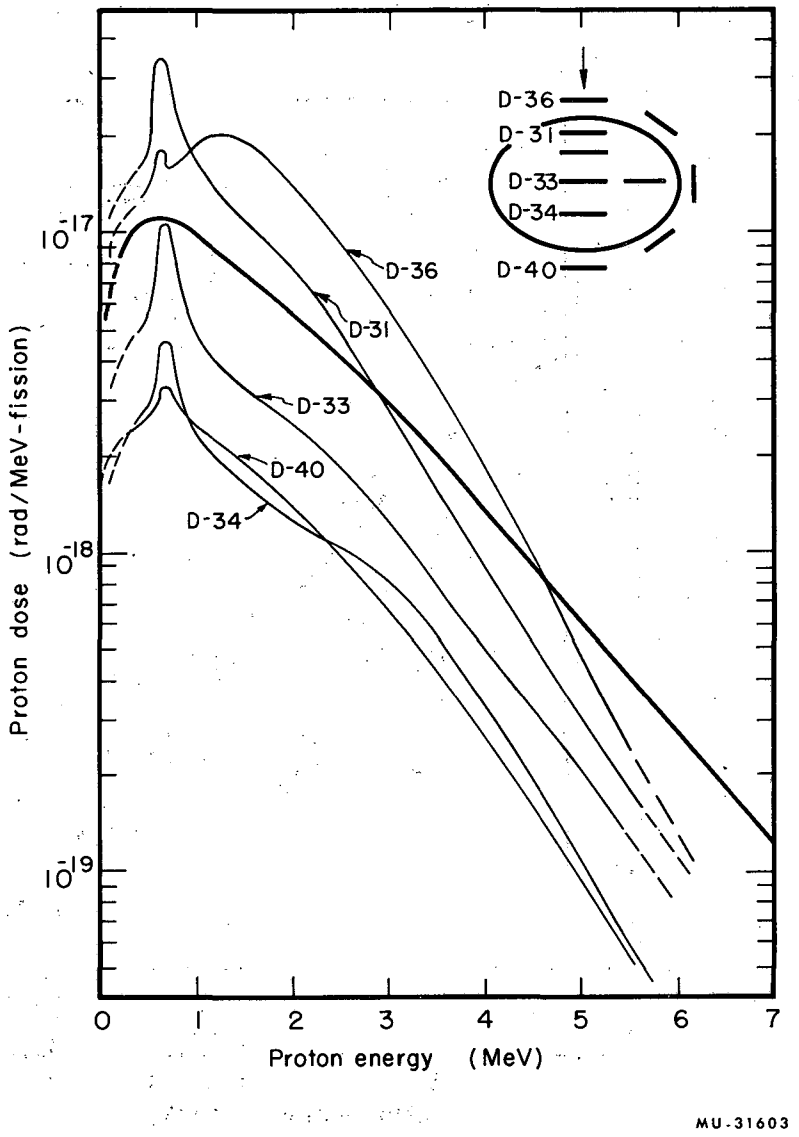
D-36
D-31
D-33
D-34
D-40
D-36
D-31
D-33
D-40
D-34
10^{-17}
10^{-18}
10^{-19}
Proton dose (rad/MeV-fission)
0
1
2
3
4
5
6
7
Proton energy (MeV)
MU-31603

Fig. 8

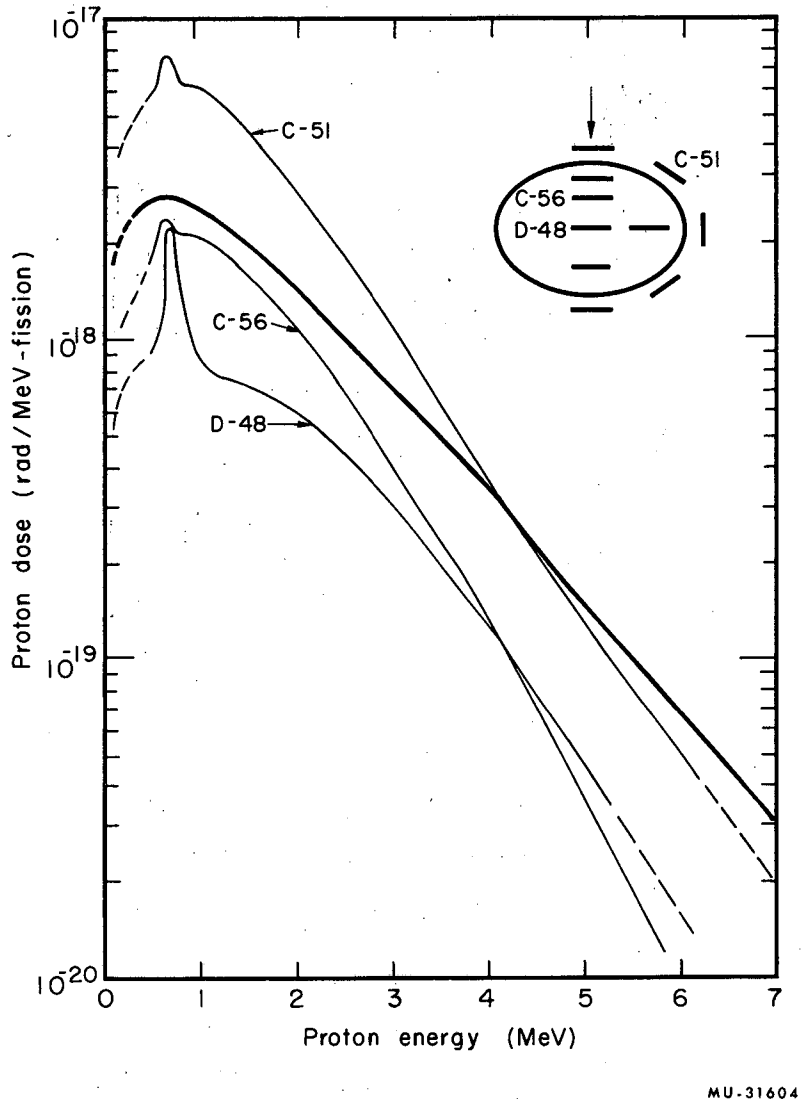
10^{-17}
10^{-18}
10^{-19}
10^{-20}
Proton dose (rad/MeV-fission)
0
1
2
3
4
5
6
7
Proton energy (MeV)
C-51
C-56
D-48
C-51
C-56
D-48
MU-31604

Fig. 9

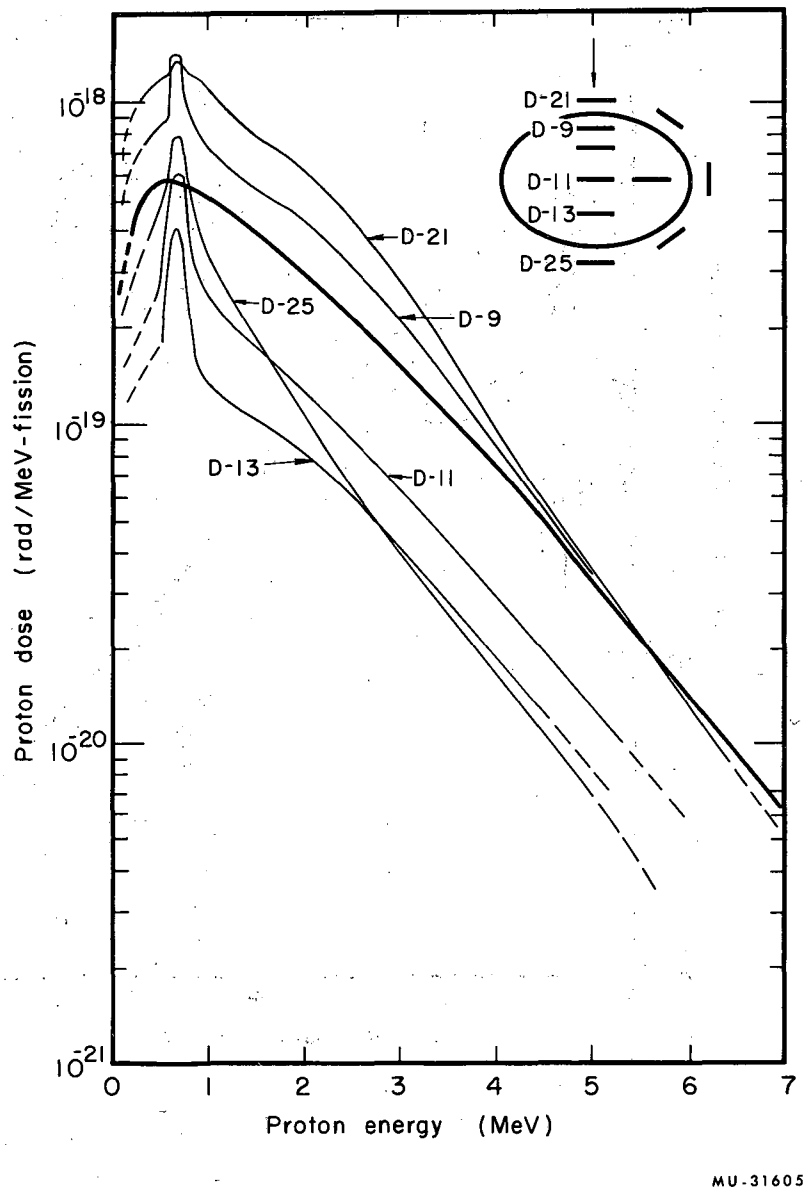
D-21
D-9
D-11
D-13
D-25
D-21
D-25
D-9
D-13
D-11
10^{-18}
10^{-19}
10^{-20}
10^{-21}
Proton dose (rad/MeV-fission)
0
1
2
3
4
5
6
7
Proton energy (MeV)
MU-31605

Fig. 10

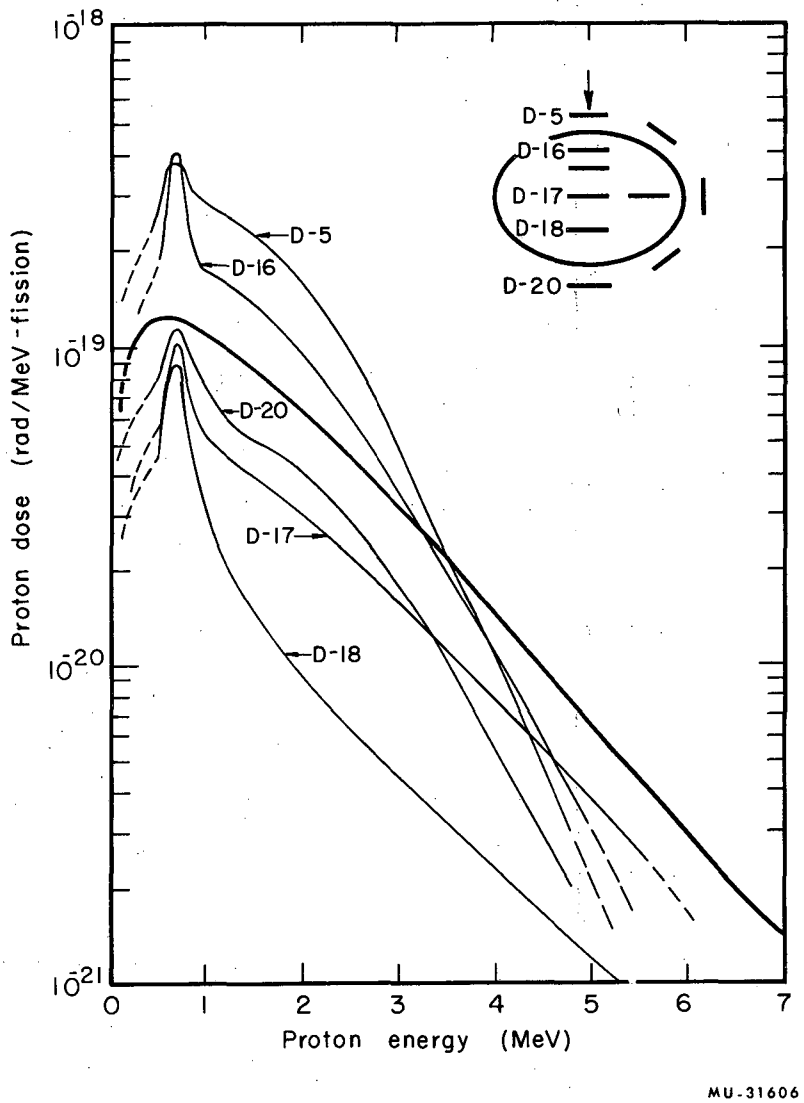
10^{-18}
10^{-19}
10^{-20}
10^{-21}
Proton dose (rad/MeV-fission)
0
1
2
3
4
5
6
7
Proton energy (MeV)
D-5
D-16
D-17
D-18
D-20
MU-31606

Fig. 11

This report was prepared as an account of Government sponsored work. Neither the United States, nor the Commission, nor any person acting on behalf of the Commission:

A. Makes any warranty or representation, expressed or implied, with respect to the accuracy, completeness, or usefulness of the information contained in this report, or that the use of any information, apparatus, method, or process disclosed in this report may not infringe privately owned rights; or

B. Assumes any liabilities with respect to the use of, or for damages resulting from the use of any information, apparatus, method, or process disclosed in this report.

As used in the above, "person acting on behalf of the Commission" includes any employee or contractor of the Commission, or employee of such contractor, to the extent that such employee or contractor of the Commission, or employee of such contractor prepares, disseminates, or provides access to, any information pursuant to his employment or contract with the Commission, or his employment with such contractor.